Research on Computer Model of Seismic Performance and Shear Bearing Capacity of Prefabricated Building Wall Structure Based on BIM

Ze Liu *

North Sichuan College of Preschool Teacher Education, Guang Yuan, China

* Corresponding Author Email: 747133007lz@sina.com

Abstract. The Markov model limited maximum likelihood algorithm is used to analyze the image. Then, the original image block and the image block affected by noise are estimated respectively. Local adaptive regression kernel and principal component analysis were used to extract feature and cluster the image block structure. The original image block's mean value and covariance matrix were computed. Subsequently, by applying weighted averaging techniques to these matrices, the noise reduction estimates for each individual image block could be achieved. The maximum likelihood method is used to make the completely confocal non-correlation, and the Markov random field model is used to limit it. This method can recover the high frequency component of the image well. The seismic response characteristics of fabricated building steel frames are studied. The results show that each group of tests follows the structural system of "block-rib-frame column triple seismic defense system", and its failure mode is one of overall shear failure. The combination of SRC frame and inclined ribbed composite shear wall can not only significantly improve its shear performance, but also obtain better damping effect.

Keywords: Prefabricated building; steel structure; layout; dense ribbed composite wall; seismic performance.

1. Introduction

Compared with ordinary cast-in-place reinforced concrete structure, prefabricated reinforced concrete structure, due to its unique natural characteristics, shows the outstanding advantages of short construction period, material consumption, low energy consumption, high efficiency, low pollution, strong bearing capacity, easy recycling, etc., is a green building layout method in the whole life cycle. It has emerged as a pivotal mechanism for the evolution and modernization of China's construction sector and the adjustment of its supply-side structure, possessing vast growth potential. The high-resolution remote sensing image reconstruction algorithms for large-scale complex scenes. Discrete Fourier transform (DFT) is used as sparse basis to [1] describe the signal of layout image. By using adaptive registration method, the plane graphic information is decoded, and the image of the plane layout of the steel structure is realized. The spatial planning of assembled buildings [2], a new compressed sensing imaging algorithm is constructed by combining and clustering the spectral information of each pixel in the image based on the correlation between spectra. The smooth 1_0 mode method is used to process the signal band of each reference pixel. By constructing a single band image without reference pixel, the measured data is compared with the measured data, and the complete image of each pixel is obtained by modifying the difference vector. The fusion algorithm that integrates high precision and non-local total variational [3]. Global gradient extraction technology is used to smooth the measured components based on the existing research. In each iteration, the smooth and textured areas are applied with high-precision total variational and non-local total variational methods until the iteration is complete, and then the smooth part is overlapped with the textured part of the edge to form a complete panorama of the prefabricated building layout. Some researchers have carried out simulation shaking table test and pseudo-dynamic experiment of 8-degree seismic reinforced dense ribbed composite shear wall. The research shows that the composite shear wall basically follows the successive failure mode of "filling block-ribbed beam-ribbed pillar-frame support", and its vibration displacement curve presents flexural shear characteristics [4]. The

self-resetting capacity was established based on the experimental results, the influence law of its shear load capacity was revealed, and the expression of its load capacity and load capacity was established. At present, researchers have combined it with traditional multi-layer reinforced concrete frame to establish a multi-layer oblique reinforced concrete frame system, and its seismic performance has been studied. Certain scholars have investigated the seismic response of framed-diagonal composite walls and discovered that their distinctive diagonal lattice configuration markedly enhances their load-bearing capability, rigidity, and energy absorption ability, while also exhibiting superior resilience and reparability.

2. Intelligent imaging research on steel structure layout of prefabricated buildings

2.1. Image processing of prefabricated steel structure layout

The original pixel points and the pixel points affected by noise in the steel structure plan of prefabricated building are estimated [5]. This project proposes an image block of composite building plane layout image block based on local adaptive regression kernel function. PCA method is used to cluster the original image block, obtain the mean value and covariance matrix of the original image block, and weighted average the image block of the obtained image block to achieve the purpose of removing noise in the image block.

Suppose M represents the number of pixels in a steel frame plan in a composite house. c_i represents the original image block in the composite house, and v_i represents the image block affected by the noise. γ_i represents the block effect between blocks of the steel structure plan in the composite building, then the estimated result $\hat{c}_i$ of c_i and v_i can be expressed by the following expression:

$$v_i = c_i + \gamma_i, i = 1, 2, \cdots, M \tag{1}$$

$$\hat{c}_i = \overline{c} + (R_{c_i}^{-1} + \sum_{j=1}^{M} \Theta_{ij} E) \sum_{j=1}^{M} \Theta_{ij} (v_i - \overline{c}) \tag{2}$$

$\overline{c}$ is the mean value and covariance matrix of the original image block c_i in the steel structure plan of the composite house, and R_{c_i} is the original image block in the composite house. Θ_{ij} is the weighting coefficient of v_i and v_j between the blocks of the steel structure plan in the composite house [6]. This project intends to replace the weighting function with the following formula (3), which replaces the weighting equation with:

$$\Theta_{ij} = \exp\left(-\frac{\| v_i - v_j \|}{\overline{c}^2} \right) / R_c^2 \tag{3}$$

Local adaptive regression kernel function is used to extract features from the blocks of the floor plan of the assembled building steel structure. PCA method is used to cluster the original image slices. In class B_t, the estimated values of the mean value, covariance matrix $\overline{c}$ and R_{c_i} of the original image slices c_i are as follows:

$$\overline{c} = A[s_i \in B_t] \approx \frac{1}{M_t} \sum_{v_i \in B_t} v_i \tag{4}$$

$$\hat{R}_{c_i} = [U]_+ \cdot r \cdot Mean(\nabla V - Mean(\nabla V)|) E \tag{5}$$

M_t represents the steel frame plan in the composite house, and the number of frames in category t. $[U]_+$ represents the matrix obtained by substituting 0 for the negative eigenvalue of the graphic pixels in the steel frame in the composite house. ∇V is the input gradient vector of the steel structure plan V in the composite building. r is a constant. By replacing the estimated values of r and $\hat{R}_{c_i}$ obtained above into formula (2), noise reduction estimation can be performed for each piece in the plane layout image of the prefabricated building steel structure [7]. However, due to many overlapping regions between each Imaging film, pixels in each Imaging film need to be fused to obtain the final estimation result and weighted average is performed to achieve the noise reduction effect of Imaging film.

$$\hat{c}_i = \sum_{r}^{R} \frac{s_{r\varphi}^{-1} \hat{c}_{r\varphi}}{\sum s_{r\varphi}^{-1}} \tag{6}$$

$$\hat{R}_{c_i} \approx (R_{c_i}^{-1} + \sum_{j=1}^{M} b_{rj} E) \tag{7}$$

R represents the number of blocks on the floor plan of the composite floor steel frame containing c_i. $\hat{c}_{r\varphi}$ represents the pixel of the φ image block above the r image block in the configuration after vectorization. $s_{r\varphi}^{-1}$ is the reciprocal of the corresponding weight of this pixel.

2.2. Intelligent imaging method for prefabricated building steel structure layout

This project intends to take the existing prefabricated building layout as the research object and the maximum likelihood method as the main research method. The three-dimensional spatial distribution information obtained by the maximum likelihood method is introduced into the three-dimensional spatial distribution information obtained by the maximum likelihood method [8]. Meanwhile, the layout diagram of the prefabricated building with its own noise is designed to be modeled twice by Markov random field method. To recover the high frequency component, the defects of the maximum likelihood method are compensated.

$P_g(u,v)$ represents the common map of the metal components in the composite house. $\otimes$ is the convolution operation symbol. Using the maximum likelihood method, the complete confocal irrelevance analysis is carried out for the steel structure layout of composite buildings

$$E_{CRM}(u,v) = L(u,v) \otimes P_g(u,v) \tag{8}$$

$L(u,v)$ is the point diffusion function of plane confocal inconsistency

The calculation formula is

$$L(u,v) = | l_1(\hat{c}_i(u), \hat{R}_{c_i}(v)|^2 \cdot \int\int_{-\infty}^{\infty} | l_2(u + \hat{c}_i(u_1), v + \hat{R}_{c_i}(v_1)|^2 \, D(u_1, v_1) du_1 dv_1 \tag{9}$$

l_1 and l_2 are the 3D point dispersion functions of the intelligent camera lens and the detection lens for the plane layout of the composite building steel structure. $D(u_1, v_1)$ stands for intelligent imaging detector function. Where u_1 and v_1 represent the radius direction of the image detection space contained in the combined building plan. The maximum likelihood algorithm can not only expand the width of the prefabricated building layout image [9]. However, its reconstructed image contains oscillating stripes, and it is difficult to obtain ideal imaging quality for the prefabricated building layout image with its own noise. An intelligent imaging method based on Markov model constraint maximum likelihood preserve the detail features and edge features, and effectively enhance the imaging effect.

$$g_{ij}^{n+1} = g^n \left[\frac{g}{L(u,v) \otimes g^n} * L(u,v) - \alpha \frac{1}{g^n} Q(g^n) \right] \tag{10}$$

g^n and g are the steel structure plane layout object image and the deterioration image of the composite building. $*$ is the intelligent associative operation of images. Where α is an intelligent image equalization parameter. $Q(g^n)$ is the energy function used to combine the house floor plan.

3. Test phenomenon and failure mode

A new design method of concrete structure based on elastic-plastic theory is presented. Although the failure characteristics of each sample are slightly different due to the difference of material and structure, the overall failure path is consistent with the law. From the loading process until the specimen produces significant cracks, this is an elastic period, because it is a fragile material, so its elastic period is very short. During this period, the test body showed significant elastic deformation characteristics, and the structure was stable without significant damage during loading. When the load of MW-1 is 1.75 mm and 4 mm, the inclined tensile crack of 45 degrees occurs, and the strength of the specimen decreases significantly. In the test, it was found that with the axial compression ratio, the MW-2 and SMW-2 blocks produced vertical fracturing at the deformation of 1 mm and 1.75 mm, but did not have significant impact on their rigidity, and then remained in an elastic state until there was a significant inflection point in the load-displacement curve, and began to enter an elastic-plastic state.

In the plastic deformation period, the cracks in the wall developed in the direction of the inclined joint at a 45-degree Angle, and the inclined joint at a 45-degree Angle, and gradually spread to the ribs, resulting in a 45-degree inclined joint in the concrete ribs, and through the corner direction of the ribs, and then after being stressed, transverse cracks were generated, the cracks became larger and larger, and scattered spalling appeared on the wall. There is also some transverse or 45-degree cracks in the frame column, and the sound of the block and concrete moving at this time can be heard.

When the load reaches the maximum value, the strength of the component decreases more significantly and gradually develops towards plasticity. With the continuous expansion of cracks in the wall and concrete, the wall is stripped from the concrete and gradually withdrawn from the working state; A large crack was generated in the steel grid and extended to the frame column. The ribbed concrete expanded; Transverse and 45-degree cracks occurred in the frame column. There are more vertical cracks in the frame column, and more vertical cracks in the east and west corners. The slippage of the steel bars and concrete is even more significant, until some of the concrete is crushed and the steel frame structure is partially destabilized. The four groups of components basically follow the "block - frame - frame - frame - structure" triple seismic defense system, and the damage characteristics are: first, the brick in the wall produces diagonal cracks, and then develops towards diagonal 45-degree cracks, the frame column diagonal cracks and a few transverse cracks, and finally leads to the overall concrete breakage and the instability of components or components. From the cracking development and failure characteristics, which is mainly manifested as shear failure.

3.1. Hysteresis performance

The transverse load is obtained by the sensor installed on the transverse actuator, and the transverse displacement is measured by the displacement meter. The transverse load-displacement hysteresis relationship is obtained through comprehensive analysis (Figure 1).

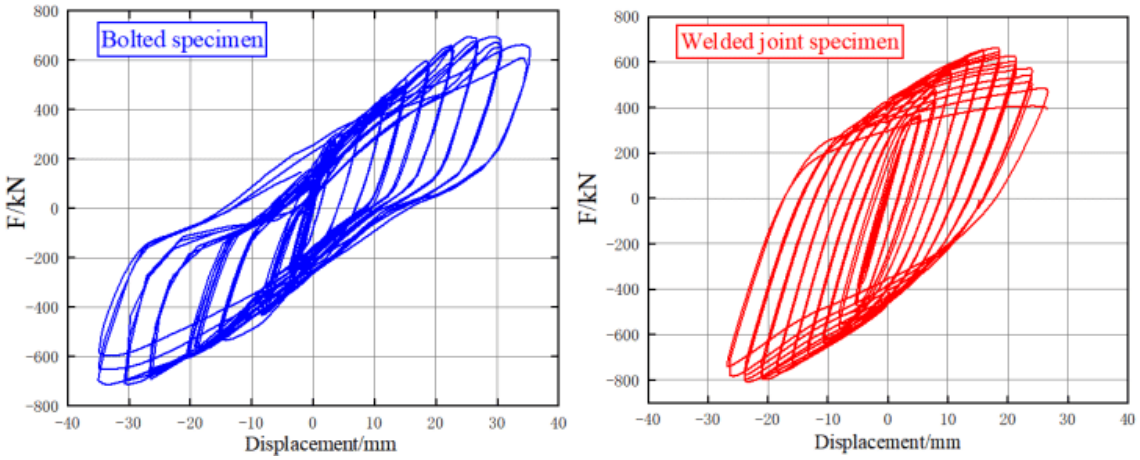

Figure 1. Hysteresis curves of each specimen.

As can be seen from the hysteresis rate curve in Figure 1, in the initial stage, the hysteresis curve is approximately a line, the loading curve is approximately the same as the unloading curve, and the stiffness does not change significantly. Moreover, the hysteresis ring is slender and the residual deformation is small, thus achieving the elastic working conditions. When the loading rate is low, the loading rate is slow and low, and the residual deformation after unloading is large, and the hysteresis rate is high, and the nonlinear performance is strong [10]. When the transverse deformation continues to increase, the hysteretic rate of concrete shows obvious compressibility, presents a "bow" type, and the area increases. After yielding, the residual deformation of concrete continues to increase, the slope gradually decreases after unloading, the hysteresis curve tends to be full, the energy consumption of the specimen increases, the hysteresis force of the material changes from the "bow" type to the inverse "S" type, and the extrusion effect becomes increasingly significant. When it reaches the limit, its residual deformation increases, hysteresis rate is higher, the covering area is larger, and it has strong energy dissipation performance, and its hysteresis rate tends to be close to the displacement axis, and forms a "Z" shape. The test results show that the middle part of the eastern frame column of MW-2 has obvious instability, and there is no obvious "Z" deformation.

3.2. Skeleton curve

The peak load points at each loading phase and the outer contour of the hysteresis loop serve as the skeletal curves for each wall specimen. (see Figure 2).

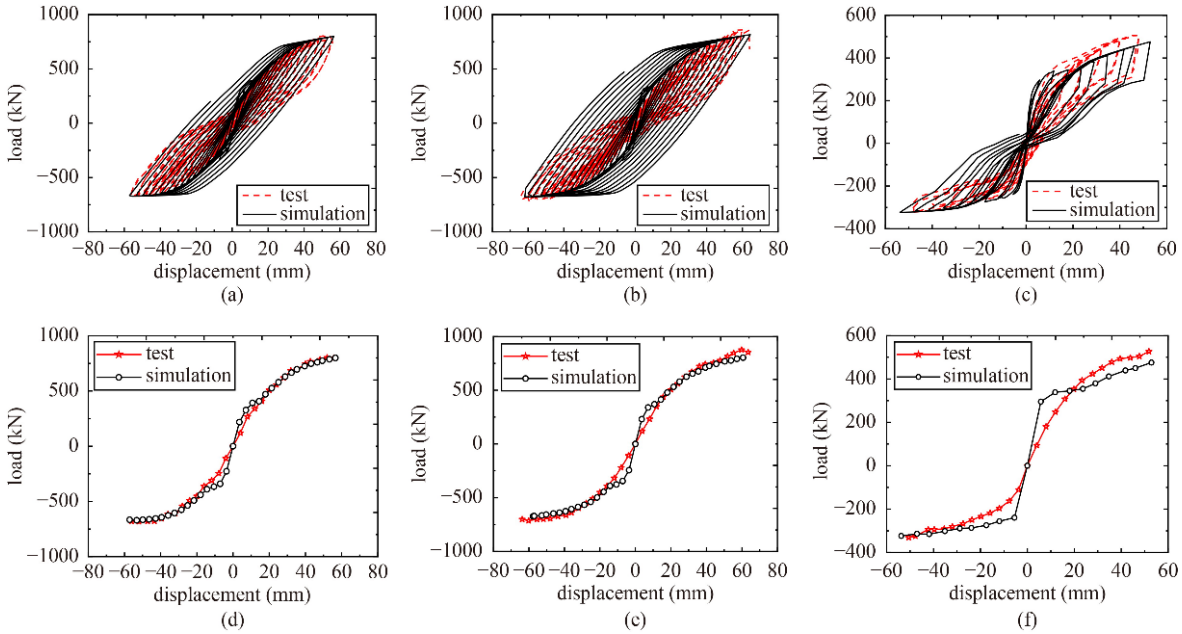

Figure 2. Skeleton curves of each specimen.

At the beginning of the test, the skeleton curve is approximately linear, and its slope is slightly different due to the difference of initial stiffness, but the difference is small [11]. After the fracture, there is a significant inflection point at the main beam, and then it enters the elastic-plastic state, which accelerates with the increase of the transverse deformation, and then increases at a slow rate until the maximum value. When the load reaches its maximum, its lateral load is reduced to 77% of the maximum load, 80% of the medium load, 70% of the SMW-1, and 86% of the SMW-2.

3.3. Bearing capacity and deformation capacity

The characteristic points in the loading process of wall specimens. The corresponding characteristic values of load and displacement are shown in Table 1. During the test, the crack has a significant inflection point on the load-displacement diagram of the sample, after which the rigidity of the sample will decrease and the determination of the crack will be clearer [12]. The yield load is obtained by using the energy equivalence method. The corresponding displacement Δ_y is the yield displacement. Peak load P_m is the maximum value of 15% failure load of the specimen, that is, $P_u = 0.85P_m$, and the value is Δ_u. In SMW-2, the failure is caused by local instability at the loading site, so the final deformation is the ultimate deformation, and the corresponding load is the failure load.

Compared with ordinary concrete member MW-1, the cracking load and yield load of steel reinforced concrete member SMW-1 are increased by 39% and 27% respectively, the peak load and failure load are increased by 38% respectively, and the maximum displacement Angle between layers is increased by 21%; The test results show SMW-2 with ordinary reinforced concrete are increased by 25% and 50% respectively, and the peak load and failure load are increased by 49% and 51% respectively, and the limit value of the interstudy displacement Angle is increased by 18%, indicating that under the same rib arrangement, the same rib arrangement is adopted. The bearing capacity and deformation performance of the composite wall of reinforced concrete are significantly improved by using section steel instead of traditional reinforced concrete.

Table 1. Load and displacement of main characteristic points of specimens.

Specimen number	Cracking point		Yield point		Peak load point		Failure point		θ_u
	P_{cr}/kN	Δ_{cr}/mm	P_y/kN	Δ_y/mm	P_m/kN	Δ_m/mm	P_u/kN	Δ_u/mm	
MW-1	58.90	1.72	91.57	3.74	100.82	20.83	85.77	28.87	1/51
MW-2	56.86	1.37	203.53	10.37	240.89	20.80	204.75	24.93	1/59
SMW-1	81.68	3.58	115.93	9.55	139.53	20.79	118.61	35.03	1/42
SMW-2	71.08	1.87	305.19	16.21	357.83	26.04	308.63	29.12	1/50

4. Conclusion

Replacing the traditional frame structure with a steel frame can not only significantly enhance its shear capacity, but also enhance its better deformation and energy dissipation, and significantly improve its seismic performance under large earthquakes. Under the condition of transverse loading, the block and lattice work together to form a common force member, while the inclined lattice structure mainly occurs in the axial displacement, which can significantly improve its lateral stiffness. Compared with the conventional orthogonal-rib structure, the shear capacity of the inclined rib structure is increased by more than 30%, the peak point stiffness is greater than 18%, and the energy dissipation performance is stronger, but it has a greater influence on the deformation performance in the later period.

References

[1] Li Wenjie. Research on seismic performance evaluation model of prefabricated shear wall structures. Journal of Guangzhou City Vocational College, vol. 15, pp.50-55, February 2021.

[2] Zheng Zhiyuan, WANG Lei, ZHANG Yujin. Research on seismic performance of prefabricated shear wall structures with external filling walls. Journal of Wuhan University of Technology, vol.45, pp.88-96, April 2023.

[3] Sun Chongfang, Chen Zhenyu, ZHAO Zhiqiang, et al. Evaluation of seismic performance of a new type slotted and unbonded horizontal joint prefabricated shear wall structure based on energy. Building Science, vol. 39, pp.8-18, September 2023.

[4] Yin Shiping, Qu Fenghao, Wang Fei, et al. Research on seismic performance and shear bearing capacity of damaged brick masonry wall strengthened by TRC. Journal of Building Structures, vol. 11, pp.107-115, February 2021.

[5] Yang Yan-Min, HU Ting-Yi, Zhang Bin-Lin, et al. Seismic performance of assembled system of sandwich wall panel and steel frame based on steel plate connection. Journal of Building Science and Engineering, vol.37, pp.109-112, March 2020.

[6] Shi Li, Wang Jie, Zhang Zuxue. Effect of aluminum powder content on mechanical properties and workability of microexpanded UHPC. Civil Engineering, vol.13, pp.72-77, February 2024.

[7] Xu Longhe, Yang Fuxiong, Chen Peng, et al. Calculation method of bearing capacity of disc spring considering the width of supporting surface. Engineering Mechanics, vol. 4, pp.1-10, January 2024.

[8] Qian Jiaru, Cui Yao, Zhang Wei, et al. Experimental study on seismic performance of composite beams of prefabricated hollow slab shear wall structures. Journal of Building Structures, vol.41, pp.102-108, January 2020.

[9] Zhao Yongqiang, Zheng Zhiyuan, Pan Han, et al. Finite element study on seismic performance of prefabricated shear wall structures considering the influence of prefabricated filled walls. Architectural Structure, vol. 52, pp.1461-1467, February 2022.

[10] Zhang Zhi-Wei. Experimental study on seismic performance of prefabricated concrete shear wall structures. Jiangxi Building Materials, vol.11, pp.50-52,58, August 2023.

[11] Ding Kewei, Zhang Yuling, Li Haodong, et al. Study on seismic performance of composite plate-steel beam assembled beam-plate joints with embedded Angle steel connectors. Journal of Anhui University of Architecture and Architecture, vol.31, pp.1-9, May 2023.

[12] Pang Rui, Wang Lu, XU Zhu, et al. Seismic performance test and bearing capacity calculation of prefabricated steel-concrete composite pipe shear wall. Building Structures, vol.50, pp.84-89, February 2020.